

Submitted to ACI Structural Journal, August 1997.

**Sensitivity of Shear Strength of RC and PC Beams
to Shear Friction and Concrete Softening
according to the MCFT**

by

Dat Duthinh

National Institute of Standards and Technology
Gaithersburg, Maryland, 20899

Ph: (301) 975-4357 Fax: (301) 869-6275

e-mail: dduthinh@nist.gov

Abstract

The Modified Compression Field Theory (MCFT) is used to study the effect of shear friction and biaxial softening on the computed shear strength of reinforced (RC) or prestressed concrete (PC) beams. A comparison is presented of the various relationships that have been proposed to represent the shear friction behavior of cracked reinforced concrete. A decrease in shear friction within the range of experimental data, as found for example in high strength concrete, can lower the shear strength of beams with minimum shear reinforcement by 15 % to 25 %, according to the MCFT.

In addition, a comparison is presented of different relationships used to represent the biaxial compression-tension strength of reinforced concrete for RC and PC beams. Some theories of biaxial softening of concrete do not predict concrete crushing even for very high deformations, but rather show significant shear force gain after stirrup yielding and crack slipping. For the RC beam example, some theories predict shear tension failure while others predict diagonal compression failure. However, the first peaks of shear load, which occur close to stirrup yielding and crack slipping are within 10% of one another for the various theories and within 10 % of the test value for the PC beam.

Introduction

The importance of aggregate interlock, or shear-friction, across shear cracks as one of the mechanisms of shear resistance in reinforced concrete (RC) beams has been recognized for quite some time (Fig. 1 adapted from MacGregor 1992 and from the Joint ASCE-ACI Task Committee 426 Report on Shear and Diagonal Tension 1973, 1990). However, traditional ACI beam design equations for shear (ACI 318-95) do not take explicit account of shear friction, but rather lump it together with other factors such as dowel effect, and the shear carrying capacity of the compressed part of the beam, into the concrete contribution term V_c .

In the last 20 years, more rational methods for shear strength calculation have been able to explicitly account for the contribution of shear friction across cracks in resisting shear. One noteworthy method, which has now been adopted in the Canadian Code (CSA A23.3-94), the Norwegian Code (NS 3473 E 1992) and the AASHTO LRFD Bridge Design Specifications (1994), is the Modified Compression Field Theory or MCFT (Vecchio and Collins 1986, Collins and Mitchell 1991).

Another aspect of shear cracks is that they also weaken the concrete struts. The presence of transverse tensile stress and strain lowers the concrete compressive strength below its uniaxial strength (softening). The MCFT provides a means to evaluate the effect of this softening on the shear strength of RC beams.

Following reviews of the MCFT, and other works on shear friction and biaxial softening, this paper presents the results of a parametric study that determines the effects of changes in shear friction and concrete softening on the shear strength of RC and PC beams, as predicted by the MCFT.

Research Significance

The shear strength of RC and PC beams remains an active area of research, especially with the advent of high strength concretes, which are beginning to exceed the data base (largely below 40 MPa) of the ACI design equations. The current ACI Code shear design equations limit f'_c to 69 MPa, although higher strength concrete is allowed, provided the minimum shear reinforcement is increased accordingly. In the last 20 years, rational methods have been developed, which incorporate the knowledge of the friction laws of shear cracks and the softening of concrete under biaxial compression and tension. This paper studies the sensitivity of the shear strength of RC and PC beams, computed according to the MCFT, to softening models and changes in shear friction, with a view of clarifying future research directions aimed at codifying the use of high strength concrete in structures.

Review of the Modified Compression Field Theory (MCFT)

The MCFT is a rational theory capable of predicting the strength of reinforced and prestressed concrete beams under shear and axial loading. It is rational in the sense that it satisfies equilibrium of forces and moments, compatibility of displacements, and the stress-strain relationships of concrete and reinforcing steel. One of the simplifying assumptions of the MCFT is that the principal directions of stress and strain coincide. According to the MCFT, the shear strength V of a RC beam is the sum of a steel contribution V_s and a concrete contribution V_c . The steel contribution is based on the variable angle (θ) truss model, whereas the concrete contribution is the shear resisted by tensile stresses f_{ct} in the diagonally cracked concrete. See Fig. 2. The concrete tensile stress f_{ct} is zero at cracks and reaches a maximum halfway between cracks. (The notation is explained in Fig. 2 and at the end of the paper).

$$V = V_s + V_c = \frac{A_v f_v}{s} jd \cot \theta + f_{ct} b_w jd \cot \theta \quad (1)$$

The concrete contribution, which depends on f_{ct} , is a function of the shear that can be transmitted across cracks by aggregate interlock. Indeed, after yielding of the transverse reinforcement, transmittal of *tension* across cracks requires local shear stresses τ along cracks. The ability of the crack interface to transmit the shear stress τ depends strongly on the crack width w . Vecchio and Collins (1986) allowed for the possibility of local *compressive* normal stress σ across cracks. Based on Walraven and Reinhardt's (1981) experimental results, they suggested the following parabolic equation to relate τ to σ (Fig. 3 from Vecchio and Collins 1986):

$$\frac{\tau}{\tau_{max}} = 0.18 + 1.64 \frac{\sigma}{\tau_{max}} - 0.82 \left(\frac{\sigma}{\tau_{max}} \right)^2 \quad (2a)$$

$$\text{with } \tau_{max} = \frac{\sqrt{f'_c}}{0.3 + \frac{24w}{c+16}} \quad \text{N, mm} \quad (2b)$$

Thus, τ_{max} , the maximum shear stress transmissible across a crack is a function of the crack width w , the concrete strength f'_c and the maximum aggregate size c . As the normal stress σ across cracks increases, so does the shear stress τ , but not quite as steeply as a linear relationship with a cohesion term.

It turns out that σ is negligible and Equation (2a) is simplified in later versions of the MCFT to (Collins and Mitchell 1991):

$$\tau = 0.18 \tau_{max} \quad (3)$$

The MCFT assumes a parabolic relationship (Hognestad 1952) to describe the stress-strain behavior of concrete in compression:

$$\frac{f_{c2}}{f_{c2max}} = 2 \left(\frac{\epsilon_2}{\epsilon_0} \right) - \left(\frac{\epsilon_2}{\epsilon_0} \right)^2 \quad (4)$$

where ϵ_0 is the strain at peak uniaxial stress and f_{c2max} , which is the compressive strength of concrete panels in biaxial tension (direction 1) - compression (direction 2), depends on the transverse tensile strain ϵ_1 . A softening parameter β is defined as the ratio of f_{c2max} to the uniaxial cylinder compressive strength f'_c . See Fig. 8b.

$$\beta = \frac{f_{c2max}}{f'_c} = \frac{1}{0.80 + 0.34 \epsilon_1 / \epsilon_0} \leq 1.0 \quad (5)$$

Equation 5 was derived from panel tests with a mean ratio of test values to equation predictions of 0.98 and a coefficient of variation for the same ratio of 0.16.

$$\text{For } \epsilon_0 = 0.002, \quad \beta = \frac{1}{0.80 + 170 \epsilon_1} \quad (6)$$

Equation 6 is used in the Canadian Code (CSA 1994). Thus, the principal compressive stress in the concrete f_{c2} is a function, not only of the principal compressive strain ϵ_2 , but also of the co-existing principal tensile strain ϵ_1 .

Review of shear friction

Walraven and Reinhardt (1981), and Walraven (1981) performed some important work on the constitutive relations of shear cracks in concrete. Their work accounts for aggregate interlock, dowel action and axial tension of the reinforcement crossing a shear crack, combines experiment and theory and shows good agreement between the two.

Direct shear tests with no bending were conducted on precracked, push-off, rectangular specimens 400 x 600 x 120 mm with a shear area of 300 x 120 mm. The two applied loads were collinear with the crack, and wedges on the upper and lower faces of the specimen channeled the loads to either side of the crack (Fig. 4). The specimens were either internally or externally reinforced, with the cube strength (f_{cc}) of concrete ranging from 20 to 56 MPa, and included a lightweight concrete and one mix with a discontinuous grading of aggregate size (no aggregate between 0.25 mm and 1.00 mm. The other mixes had a distribution of aggregate sizes). The reinforcement ranged in ratio from 0.56% to 3.35% and in inclination from 45° to 135° to the crack plane. In one series of experiments, the reinforcement bars were covered with soft sleeves extending 20 mm on both sides of the crack to eliminate dowel action. During the tests, crack displacements were recorded versus the applied shear force. In addition, for the externally reinforced specimens, the (normal) restraint force exerted by the reinforcement crossing the plane of the crack was measured. Thus, curves of shear stress and normal stress versus crack slip for various values of crack width could be plotted for the externally reinforced specimens (Fig. 5). Walraven and Reinhardt (1981) noticed that the behavior of the internally reinforced specimens was totally different from that of the externally reinforced ones. The crack displacement path (curve of crack width versus crack slip) was much more sensitive to the stiffness of the reinforcement for the externally reinforced specimens than for the internally reinforced ones. Nevertheless, Walraven and Reinhardt used the same model of aggregate interlock for both types of specimens. In addition to aggregate interlock, the shear crack model of the internally reinforced specimens also included the dowel action of the reinforcement and its bond to concrete.

The analytical model of aggregate interlock assumes the concrete to be composed of two phases: a rigid, perfectly plastic mortar and rigid spherical aggregates of various sizes (Fig. 5b). Knowing the volumetric ratio of aggregate to concrete and the size distribution of the aggregate, one can work out the average number of aggregate particles encountered by a crack of a given length. The portion of the mortar that interferes geometrically with the aggregate when the crack faces open and slide with respect to one another is assumed to yield, thus engendering normal and shear stresses which are related by a coefficient of friction μ . Equilibrium is related to frictional sliding and crushing of matrix material along the projected contact areas A_x and A_y . These depend on the crack slip v and opening w and the mix proportions (maximum aggregate size and volumetric percentage of aggregate). The constitutive equations for the analytical model of the cracked specimens are:

$$\sigma = \sigma_{pu} (A_x - \mu A_y) \quad \text{and} \quad \tau = \sigma_{pu} (A_y + \mu A_x) \quad (7)$$

where $A_x = \sum a_x$ and $A_y = \sum a_y$ depend on the crack width w , the crack slip v , the maximum particle diameter c and the total aggregate volume per unit volume of concrete (Fig. 5b and c). The strength of the mortar σ_{pu} , assumed to be elastic-perfectly plastic (Fig. 5a), and the coefficient of friction μ

between mortar and aggregate were found from fitting curves to the experimental results:

$$\mu = 0.40 \text{ and } \sigma_{pu} = 6.39 f_{cc}^{0.56} \text{ in MPa} \quad (8)$$

Physically reasonable values can be found that fit *all* experimental curves well, thus lending credibility to the theory. (The indeterminacy of the *two* parameters μ and σ_{pu} in Eq. 7 means that *two* curves such as those shown in Fig. 5d can always be fitted well. The credibility of the theory lies in the good fit of *all* the curves.)

After performing further tests of 88 push-off, internally reinforced specimens with compressive strengths ranging from 17 to 60 MPa, Walraven, Fréney and Puijssers (1987) developed the following empirical expression for the shear friction capacity of internally reinforced cracks as a function of concrete strength and amount of reinforcement, but not of aggregate size :

$$\tau_{max} = C_1 (\rho_v f_y)^{C_2} \quad (9)$$

in which

$$C_1 = 0.822 f_{cc}^{0.406} \text{ and } C_2 = 0.159 f_{cc}^{0.303} \text{ in MPa}$$

f_{cc} is the concrete compressive strength of 150 mm cubes, and ρ_v and f_y are the cross-sectional area ratio and yield strength of the shear reinforcement. Comparison between theoretical values of τ_{max} according to Eq. 9 and experimental results by Hofbeck, Ibrahim and Mattock (1969), Walraven and Reinhardt (1981), Fréney (1985), Puijssers and Liqui Lung (1985) produced excellent agreement (mean of 1.001 and standard deviation of 0.109 for the ratio experimental / theoretical values).

Mau and Hsu's formula (1988) works well for the shear capacity of cracks in normal strength reinforced concrete:

$$\frac{\tau_{max}}{f'_c} = 0.66 \sqrt{\omega} < 0.3 \quad \text{with} \quad \omega = \frac{\rho_v f_y}{f'_c} \quad (10)$$

When applied to the same test results, Eq. 10 performed almost as well as Eq. 9 and is much simpler to use (mean = 1.019, standard deviation = 0.127 for the ratio experimental / theoretical values). Again, aggregate size is not a factor.

Since crack surfaces are smoother in high strength concrete (HSC) than in normal strength concrete (NSC) – cracks tend to go through the aggregate in HSC whereas they go around the aggregate in NSC – one would expect a decrease in shear friction as the concrete strength increases. This is indeed the case, as was borne out by shear friction tests on precracked, push-off specimens made of concrete with a cylinder strength of 100 MPa or a cube strength of 115 MPa (Fréney et al. 1987, Walraven and Stroband 1994, Walraven 1995). Shear-friction at a given crack slip and opening for HSC (say 100 MPa) is reduced to 35% of its value for NSC (say 40-60 MPa) for externally reinforced specimens, and in the range of 55% - 75% for internally reinforced ones. The constitutive equations of the model for cracks in HSC are then:

$$\sigma = k \sigma_{pu} (A_x - \mu A_y) \quad \text{and} \quad \tau = k \sigma_{pu} (A_y + \mu A_x) \quad (11)$$

with $k = 0.35$ for externally reinforced HSC and $k = 0.65$ for internally reinforced HSC.

Besides the MCFT, other theories of beam shear strength also use Walraven's experimental results to account for shear friction. Reineck (1982, 1991) used the following constitutive equations for the friction of crack faces:

$$\tau = \tau_{f0} + 1.7 \sigma = \tau_{f0} \frac{v - 0.24 w}{0.096 w + 0.01} \quad \text{MPa, mm} \quad (12)$$

The cohesion friction stress τ_{f0} is the limiting value of shear strength without normal stress σ on the crack face:

$$\tau_{f0} = 0.45 f_t \left(1 - \frac{w}{0.9} \right) \quad \text{MPa, mm} \quad (13)$$

where f_t is the concrete tensile strength.

Kupfer and Bulicek (1991) used the following relationships from Walraven and Reinhardt (1981):

$$\begin{aligned} \tau &= -\frac{f_{cc}}{30} + \left(1.8 w^{-0.8} + (0.234 w^{-0.707} - 0.20) f_{cc} \right) v \geq 0 \\ \sigma &= \frac{f_{cc}}{20} - \left(1.35 w^{-0.63} + (0.191 w^{-0.552} - 0.15) f_{cc} \right) v \leq 0 \end{aligned} \quad (14)$$

where the units are MPa and mm.

Earlier, Kupfer, Mang and Karavesyoglou (1983) used:

$$\begin{aligned} \frac{\tau}{f'_c} &= 0.117 - 0.085 v & \text{for case a: } v = w \\ \frac{\tau}{f'_c} &= 0.017 + 0.1 \frac{v}{w} - 0.085 v & \text{for case b: } v \neq w \end{aligned} \quad (15)$$

These equations were based on earlier work by Walraven and derived from experiments performed on concrete with compressive strength of 25 MPa and for $v > 0.20$ mm. In beams, case (a) arises when the average strain of both flanges equals the longitudinal component of the normal strain of the compression struts. This situation occurs in prestressed beams. In case (b), the average strain of both chords is zero.

Poli, Prisco and Gambarova (1990) used a "rough crack model" (Bažant and Gambarova, 1980) to describe aggregate interlock in their theory of beam shear strength:

$$\begin{aligned} \sigma &= 0.62 \frac{r \sqrt{w} \tau}{(1 + r^2)^{0.25}} \quad \text{N-mm units} \\ \tau &= 0.25 f'_c \left(1 - \sqrt{\frac{2w}{c}} \right) r \frac{a_3 + a_4 |r|^3}{1 + a_4 r^4} \end{aligned} \quad (16)$$

where

$$a_3 = 9.8 / f'_c \quad a_4 = 2.44 - 39 / f'_c \quad \text{and} \quad r = v / w .$$

In earlier work based on tests by Paulay and Loeber (1974), Bažant and Gambarova (1980) suggested the following formulas, which were later updated to Eq. 16, for shear stress τ and normal compressive stress σ in cracks of concrete members, as functions of crack opening w and slip v :

$$\sigma = - \frac{0.534}{1000 w} (145 |\tau|)^p \quad \text{and} \quad \tau = \tau_{max} r \frac{a_3 + a_4 |r|^3}{1 + a_4 r^4} \quad \text{N-mm units} \quad (17)$$

with $\tau_{max} = 0.245 f'_c \frac{c^2}{c^2 + 100 w^2}$ and $p = 1.30 \left(1 - \frac{0.231}{1 + 0.185 w + 5.63 w^2} \right)$

where

$$a_3 = 10 / f'_c \quad a_4 = 2.44 - 39.8 / f'_c \quad \text{and} \quad r = v / w .$$

A comparison of various relationships for shear and normal stresses versus crack slip for two crack openings ($w = 0.5$ or 0.8 mm) is shown in Fig. 6. The curves are based on $f_{cc} = 59$ MPa, $f'_c = 50.2$ MPa, $f_t = 3.5$ MPa, and $c = 16$ mm. Also shown are experimental data from Walraven and Reinhardt (1981). The following can be observed:

- Walraven and Reinhardt's (1981) Eqs. 14 are a good approximation of their experimental data in the linear range. However, the equations need to have a cap so shear and normal stresses do not increase indefinitely as crack slip increases.
- Reineck's (1991) Eqs. 12 and 13 also need to have a cap. They approximate the experimental data well for a crack width of $w = 0.5$ mm, but not for $w = 0.8$ mm .
- Poli, Prisco and Gambarova 's (1990) Eqs. 16 and Bažant and Gambarova 's (1980) Eqs. 17 follow the general trend of the data, but there are significant deviations from Walraven's experimental data. A fine tuning of the parameters of the models could bring better agreement.
- Kupfer, Mang and Karavesyrogrou's (1983) Eq. 15b is based on weaker concrete and does not agree well with Walraven and Reinhardt's (1981) experimental data.

Review of Concrete Softening

The web of reinforced concrete beams under shear is in a state of biaxial tension-compression. The presence of simultaneous transverse tensile strain leads to a deterioration of the compressive strength of cracked concrete (Fig. 7). This softening behavior has been investigated in panel tests.

Vecchio and Collins (1993) reviewed various models of compression softening of cracked reinforced concrete panels due to transverse tension. The following is adapted from their review. In an early

study, Vecchio and Collins (1982) expressed β as a function of the ratio of the principal strains:

$$\beta = \frac{1}{0.85 - 0.27 \varepsilon_1/\varepsilon_2} \quad (18)$$

where ε_1 is the principal tensile strain, averaged over several cracks. Vecchio and Collins used Hognestad's (1952) parabola for the uniaxial compressive stress-strain curve of concrete. Both peak stress f'_c and its associated strain ε_0 were multiplied by β (Fig. 8a). Good agreement was found with 178 experimental data points (mean ratio = 1.01, coefficient of variation = 0.15).

Kollegger and Mehlhorn (1987, 1990) concluded that the effective compressive strength did not reduce beyond $0.8f'_c$ and that the prime influencing factor appeared to be the principal tensile stress f_{c1} rather than the principal tensile strain ε_1 . The value of β was given as follows, for different values of normalized tensile stress:

$$\begin{aligned} \text{for } 0 \leq f_{c1}/f_t \leq 0.25, & \quad \beta = 1.0 \\ \text{for } 0.25 < f_{c1}/f_t < 0.75, & \quad \beta = 1.1 - 0.4 f_{c1}/f_t \\ \text{and for } 0.75 \leq f_{c1}/f_t \leq 1.0, & \quad \beta = 0.8. \end{aligned} \quad (19)$$

They based their conclusions on 55 panel tests which had the tension-compression loads applied parallel to the reinforcement in most tests, but with some applied at 45° .

Miyahara et al.(1988) proposed a softening model based on the principal tensile strain:

$$\begin{aligned} \text{for } \varepsilon_1 \leq 0.0012, & \quad \beta = 1.0 \\ \text{for } 0.0012 < \varepsilon_1 < 0.0044, & \quad \beta = 1.15 - 125 \varepsilon_1 \\ \text{and for } 0.0044 \leq \varepsilon_1, & \quad \beta = 0.60. \end{aligned} \quad (20)$$

The degree of softening is much less than that predicted by Vecchio and Collins.

Shirai and Noguchi (1989) and Mikame et al. (1991) proposed the following relationship for the softening parameter:

$$\beta = \frac{1}{0.27 + 0.96 (\varepsilon_1/\varepsilon_0)^{0.167}} \quad (21)$$

They noted that the softening is greater for HSC than for NSC.

For HSC, Ueda et al.(1991) proposed the following:

$$\beta = \frac{1}{0.8 + 0.6 (1000 \varepsilon_1 + 0.2)^{0.39}} \quad (22)$$

Vecchio and Collins (1993) updated their model as follows: their new base uniaxial stress-strain curve is the Thorenfeldt (1987) curve (Fig. 8c), which is more appropriate for HSC (more linear in its pre-ultimate response) than Hognestad's parabola (Fig. 8a). The parameters for the Thorenfeldt curve

were determined by Collins and Porasz (1989):

$$f_{c2base} = -f_p \frac{n(-\epsilon_2/\epsilon_p)}{n-1 + (-\epsilon_2/\epsilon_p)^{nk}} \quad (23)$$

$$\begin{aligned} \text{where } n &= 0.80 + f_p / 17 \text{ (MPa)} \\ k &= 1.0 && \text{for } -\epsilon_p < \epsilon_2 < 0, \\ k &= 0.67 + f_p / 62 \text{ (MPa)} && \text{for } \epsilon_2 < -\epsilon_p, \\ f_p &= \text{maximum compressive stress for softened concrete} \end{aligned} \quad (24)$$

Equations 23 and 24 are used with $f_p = \beta f_c'$ and $\epsilon_p = \epsilon_0 =$ strain in uniaxial compression at peak stress f_c' . The base stress-strain curve is modified in two possible ways:

Model A uses strength and strain softening, i.e., both peak stress and its corresponding strain decrease (Fig. 8c):

$$\beta = \frac{1}{1.0 + K_c K_f} \quad (25)$$

$$\text{where } K_c = 0.35 \left(\frac{-\epsilon_1}{\epsilon_2} - 0.28 \right)^{0.80} \geq 1.0 \quad \text{for } \epsilon_1 < \epsilon_{1L}, \quad \text{and}$$

$$K_f = 0.1825 \sqrt{f_c'} \text{ (MPa)} \geq 1.0.$$

ϵ_{1L} is the limiting tensile strain in the concrete at which the reinforcement at a crack begins to yield and the concrete suffers little additional cracking. The curve is divided into three parts:

Pre-peak: For $-\epsilon_2 < \beta\epsilon_0$, f_{c2} is calculated from Eq. 23 with $f_p = \beta f_c'$ and $\epsilon_p = \beta\epsilon_0$;

Peak: For $\beta\epsilon_0 \leq -\epsilon_2 \leq \epsilon_0$, $f_{c2} = f_p = \beta f_c'$; and

Post-peak: For $-\epsilon_2 > \epsilon_0$, $f_{c2} = \beta f_{c2base}$ with f_{c2base} calculated from Eq. 23 using $f_p = f_c'$ and $\epsilon_p = \epsilon_0$.

Note that $K_f \geq 1$ for $f_c' \geq 30$ MPa and $K_c \geq 1$ for $-\epsilon_1 / \epsilon_2 \geq 4$.

Model B uses strength only softening (Fig. 8d):

$$\beta = \frac{1}{1 + K_c} \quad \text{where } K_c = 0.27 \left(\frac{\epsilon_1}{\epsilon_0} - 0.37 \right) \quad (26)$$

In a later update, Vecchio, Collins and Aspiotis (1994) conducted 12 shear tests of panels 890 mm \times 890 mm \times 70 mm made of 55 MPa concrete. The panels were reinforced by two orthogonal grids at 45° to their edges. Results show that the compression-softening formulation developed for normal strength concrete elements apply equally well to HSC elements. Now Model B also has a K_f factor:

$$K_f = 2.55 - 0.2629 \sqrt{f_c'} \text{ (MPa)} \leq 1.11 \quad (27)$$

Both models agree well with experiments, with the updated Model B being slightly superior.

Belarbi and Hsu (1991) also used Hognestad's parabola as a basis and suggested one softening parameter for stress and another for strain:

$$\beta_\sigma = \frac{0.9}{\sqrt{1 + K_\sigma \varepsilon_1}} \quad \text{and} \quad \beta_\varepsilon = \frac{1}{\sqrt{1 + K_\varepsilon \varepsilon_1}} \quad (28)$$

where K_σ and K_ε depend on the orientation ϕ of the cracks to the reinforcement and the type of loading in the biaxial test as follows:

ϕ	Proportional Loading		Sequential Loading	
	K_σ	K_ε	K_σ	K_ε
45°	400	160	400	160
90°	400	550	250	0

In a later paper, Belarbi and Hsu (1995) presented the results of tests of 22 panels 1400 x 1400 x 178 mm under biaxial tension-compression. The panels had a concrete strength of 40 MPa, minimal reinforcement (0.54%) in the compression (transverse) direction and various reinforcement ratios in the tension (longitudinal) direction. For a non-softened, standard cylinder, stress is a parabolic function of strain as in Hognestad's equation. The following stress-strain relationship is proposed for softening (see Fig. 8a):

$$\begin{aligned} \text{For } \varepsilon_2 \leq \beta \varepsilon_0 \quad f_{c2} &= \beta f'_c \left[2 \left(\frac{\varepsilon_2}{\beta \varepsilon_0} \right) - \left(\frac{\varepsilon_2}{\beta \varepsilon_0} \right)^2 \right] \\ \text{For } \varepsilon_2 > \beta \varepsilon_0 \quad f_{c2} &= \beta f'_c \left[1 - \left(\frac{\frac{\varepsilon_2}{\beta \varepsilon_0} - 1}{\frac{2}{\beta} - 1} \right)^2 \right] \\ \beta &= \frac{0.9}{\sqrt{1 + K_\sigma \varepsilon_1}} \end{aligned} \quad (29)$$

where $K_\sigma = 400$ for proportional loading,

250 for sequential loading with some tension release just prior to failure.

$K_\sigma = 400$ is usually chosen for structural elements. This softening is less severe than that proposed by Vecchio and Collins (1986). This may be attributed to the orientation of the reinforcements: 45° to the principal directions for Vecchio and Collins and parallel to the principal directions for Belarbi and Hsu (1995). The amount of reinforcement, especially transverse, is therefore also different between Vecchio and Collins on the one hand and Belarbi and Hsu on the other.

Tanabe and Wu (1991) presented some Japanese experimental results for biaxial tension-compression and the corresponding softening coefficient. Maekawa and Okamura proposed the following softening coefficient, based on measurements of reinforced cylindrical specimens under axial compression and internal pressure:

$$\begin{aligned}
\beta &= 1.0 && \text{for } \epsilon_1 < \epsilon_a \\
\beta &= 1.0 - 0.4 \frac{\epsilon_1 - \epsilon_a}{\epsilon_b \rho^2 \epsilon_a} && \text{for } \epsilon_a \leq \epsilon_1 \leq \epsilon_b \\
\beta &= 0.6 && \text{for } \epsilon_b < \epsilon_1
\end{aligned} \tag{30}$$

where $\epsilon_a = 0.0012$ and $\epsilon_b = 0.0044$.

Shirai performed tests of small reinforced panels and proposed:

$$\begin{aligned}
\beta_1 &= - \left(\frac{0.31}{\pi} \right) \tan^{-1} (4820 \epsilon_1 - 11.82) + 0.84 \\
\beta_2 &= -5.9 \frac{\sigma_1}{f'_c} + 1.0 \\
\beta &= \beta_1 * \beta_2
\end{aligned} \tag{31}$$

Some researchers have opted for a constant softening factor. Kupfer, Mang and Karavesyoglou (1983) used an experimental softening factor of 0.85 coupled with a sustained load factor of 0.80:

$$f_{c2} = 0.80 \times 0.85 \times f'_c \approx \frac{2}{3} f'_c \tag{32}$$

Kupfer and Bulicek (1991) used:

$$f_{c2} = f'_c \times 0.85 \times 0.75 \left(1 - \frac{f'_c}{250} \right) \text{ MPa} \tag{33}$$

where 0.85 = factor for sustained load,
0.75 = factor for irregular crack trajectory, and
 $(1 - f'_c/250)$ = difference between cylinder strength and uncracked concrete prism.

For Reineck (1982, 1991) the strength of the web struts is not lower than

$$f_{cw} = 0.80 f'_c. \tag{34}$$

In a recent paper on beam shear strength, Prisco and Gambarova (1995) used Hsu's (1993) formulation. To account for the effects of transverse reinforcement in tension, the concrete strength is reduced in one of two possible ways:

$$\begin{aligned}
f_c &= 0.75 f'_c \\
\text{or } f_c &= \frac{0.9 f'_c}{\sqrt{1 + 600 \epsilon_1}} \geq \frac{f'_c}{2}
\end{aligned} \tag{35}$$

As can be seen from the wide variety of formulations, a consensus has yet to be reached among researchers on whether the concrete softening parameter is constant, or dependent on the average principal tensile stress or strain. The question this paper addresses is, how do these various formulations affect beam shear strength. The tool used for this purpose is the MCFT.

Parametric Study

As mentioned in the preceding review, the MCFT accounts for shear transfer across cracks, and concrete softening due to the biaxial state of tension-compression in the web of beams loaded in shear. Since many different formulations for shear friction and concrete softening exist, a parametric study is performed using the MCFT to determine the influence of these two factors on beam shear strength. For this purpose, the computer program "SHEAR" and two example beams (Fig. 9) are adapted from Collins and Mitchell (1991). SHEAR can predict the load-deformation response of reinforced or prestressed concrete beams subjected to shear or shear combined with axial load. At each step, the user inputs a value of principal tensile strain ϵ_1 and the program assumes a strut angle θ , then computes strains, loads, crack widths, etc. according to a 17-step procedure used by Collins and Mitchell (1991) to implement the MCFT. In particular, Eqs. 3, 4 and 6 are coded into SHEAR. If convergence is not achieved, another value of θ is tried. The program stops when equilibrium cannot be achieved after a specified number of iterations, due to concrete crushing or all reinforcement yielding.

Table 1: Measured and Predicted Shear Strength (kN) of PC Beam CF1

	Support Face	$h/2$ away	Midspan
TEST	430		
SHEAR			473
ACI	443	498	
RESPONSE	342	400	
DUALSECTION	369	423	
AASHTO	373	389	

The base case ($F = \tau / \tau_{max} = 0.18$, $\rho_v = 0.61\%$) corresponds to a PC beam tested by Arbesman and Conte (Fig. 9a, b) and used as an example by Collins and Mitchell (1991). The measured strength of the beam was 430 kN versus a prediction of 473 kN by SHEAR, which only accounts for shear and axial forces, but not bending. The result of SHEAR would hold here for the middle of the test span where the bending moment is zero, and is therefore comparable to the ACI sum of web-shear cracking and stirrup capacity, $V_{cw} + V_s = 325 + 173 = 498$ kN. This value would apply here to a section at a distance $h/2$ of half the section depth from the support face. On the other hand, at the support face of the test span - moments are highest at the support and at load $2P$ - the ACI sum of flexure-shear cracking and stirrup capacity, $V_{ci} + V_s = 270 + 173 = 443$ kN, provides a good

prediction of the failure shear load and the location of the failed section. More refined versions of the MCFT have been implemented in computer programs capable of handling shear, axial forces and bending moments. RESPONSE predicts a shear strength of 342 kN at the support face and 400 kN a distance $h/2$ away. The more accurate DUALSECTION predicts a shear strength of 369 kN at the support face and 423 kN a distance $h/2$ away. The AASHTO tables, which are based on the MCFT, predict a shear strength of 373 kN at the support face and 389 kN a distance $h/2$ away. See Table 1.

Shear Friction

As mentioned above, shear friction enters into the MCFT as a parameter $F = \tau / \tau_{max} = 0.18$ with τ_{max} a function of crack width w and maximum aggregate size c (Eqs. 2b and 3). This shear friction parameter was varied from a low value of $0.35 \times 0.18 = 0.063$ to a high value of $1.5 \times 0.18 = 0.27$. Computer program SHEAR was modified by varying F .

Shear Friction of PC Beams

Fig. 10a, b and c show the computed shear force V versus crack width w relationship for a concrete strength of $f'_c = 38.6$ MPa, various combinations of shear friction parameter ($F = 0.063, 0.18, \text{ or } 0.27$), and area of shear reinforcement ($\rho_v = 0.12\%, 0.28\%, 0.61\%, \text{ or } 1.11\%$). The shear reinforcement uses #2 bars (smooth, $\phi = 6$ mm) at 355 mm or 152 mm spacing, #3 or #4 bars (deformed, $\phi = 9.5$ or 13 mm) at 152 mm spacing. As the shear reinforcement varies, so does its crack control characteristics (s_{mx}, s_{mv}) which must be input into the program (Table 2). The shear reinforcement obeys ACI design guidelines:

Table 2 Stirrup and Crack Spacing for PC Beam

Stirrup bar #	s mm	ρ_v %	s_{mx} mm	s_{mv} mm
2 (smooth)	355	0.12	414	1252
2 (smooth)	152	0.28	414	602
3	152	0.61	414	295
4	152	1.11	414	246

Maximum shear reinforcement ratio (ACI § 11.5.6.8):

$$\rho_v = \frac{A_v}{b_w s} \leq \frac{8 \sqrt{f'_c}}{f_y} \quad \text{lb, inch system}$$

$$\text{or } \rho_v = \frac{A_v}{b_w s} \leq \frac{0.7 \sqrt{f'_c}}{f_y} = \frac{0.7 \sqrt{38.6}}{367} = 1.2 \% \quad \text{N, mm system}$$

Maximum stirrup spacing (ACI § 11.5.5.4):

$$s \leq \frac{A_v f_y}{f_{pu} A_{ps}} \frac{80}{d} \sqrt{\frac{b_w}{d}} \quad \text{lb, inch or N, mm systems}$$

$$s \leq \frac{64.5 \times 367}{1682} \frac{80}{926} 559 \sqrt{\frac{152}{559}} = 355 \text{ mm}$$

or (ACI § 11.5.4.1):

$$s \leq 0.75 h = 0.75 \times 610 = 457 \text{ mm}$$

Minimum shear reinforcement:

$$\rho_v \geq \frac{50}{f_y} \quad \text{lb, inch system}$$

$$\text{or } \rho_v \geq \frac{0.345}{f_y} = \frac{0.345}{367} = 0.094 \% \quad \text{N, mm system}$$

In all cases, failure was by shear compression (concrete crushes, symbol *c* in curves), preceded by stirrup yielding (symbol *y*) and crack slipping (symbol *s*). The program was run until failure, even after crack widths had reached unrealistic values (the range of shear friction laws only extends to $w \leq 1.5$ mm), to show the increase in ductility as the amount of shear reinforcement or the shear friction parameter decreases. Also, as crack widths increase, the *V-w* curves for various friction parameters approach one another, as they should, since shear friction approaches zero. Two types of behavior can be observed:

- For high and medium shear reinforcement ratio ($\rho_v > 0.3$ %, Fig. 10b), the curve *V-w* typically follows a linear path up to stirrup yielding or crack slipping. The latter occurs when tension in the concrete reaches a limit imposed by the shear reinforcement and shear friction across cracks:

$$f_{limit} = v_{ci} \tan \theta + \frac{A_v}{b_w s} (f_{vy} - f_v)$$

For high friction, stirrups yield before cracks slip; for low friction, the order is reversed; and for medium friction, stirrup yielding and crack slipping occur simultaneously. Peaks of shear force *V* occur at initiation of crack slipping, although for low friction, it's only a local peak (*V* in this case reaches its global peak at large crack widths $w > 2$ mm).

- For low shear reinforcement, the shear force reaches a peak at a small crack width ($w < 0.05$ mm), then drops precipitously when concrete starts to crack. For $\rho_v = 0.28$ %, after the initial drop, the load recovers and increases to a maximum until cracks start to slip, at which point, it starts to decrease (Fig. 10c). For $\rho_v = 0.28$ % and low friction, and for $\rho_v = 0.12$ %, there is no load increase after the initial sharp drop at initial cracking. However, for $\rho_v = 0.12$ % and high or medium friction, a change of slope is still noticeable at initial crack slip.

Table 3 Variation of Shear Force V of a PC Beam for Various Values of Shear Friction F and Stirrup Ratio ρ_v .

F	0.27			0.18			0.063			Method
	ρ_v %	θ°	V (kN)	%	θ°	V (kN)	%	θ°	V (kN)	
1.11	29.3	653.1	103	29.5*	632.7*	100	28.6*	602.2*	95	1 mm offset
	30.9	646.7	100	30.9*	645.0*	100	29.9*	593.4*	92	linear limit
	29.5	655.7	102	30.9*	645.0*	100	28.3*	604.5*	94	peak
0.61	24.3	477.3	105	23.9	456.5	100	23.2	428.3	94	1 mm offset
	26.8	492.8	104	26.5	472.8	100	25.6	414.1	88	linear limit
	25.8	500.5	106	26.5	472.8	100	22.7	429.7	91	peak
0.28	20.8	318.7	107	20.5	297.3	100	19.9	261.8	88	1 mm offset
	21.6	329.6	111	20.5	297.3	100	19.0	258.0	87	$w = 1$ mm
	22.6	348.9	109	22.2	321.0	100	22.4	281.1	86	peak
0.12	17.2	222.2	110	16.4	201.5	100	14.9	169.3	84	1 mm offset
	18.0	234.3	116	16.4	201.5	100	14.2	163.6	81	$w = 1$ mm
	21.5	284.3	97	22.6	292.1	100	17.1	194.7	67	slope change

* Results obtained using Eq. 2 or Eq. 3.

Because the shapes of the V - w curves vary (Fig. 10b, c), several methods are used to compare them:

- Peaks of V are used. For $\rho_v = 0.12$ %, “peaks” degenerate to points of sudden change in negative slope.
- Values of V at $w = 1$ mm are selected.
- Where a linear part exists (prior to crack slipping or stirrup yielding), the values of V at the end of the linear range are selected.
- Intersections of the curves with a straight line parallel but offset with respect to the linear part by $w = 1$ mm are also used.
- Finally, where a linear part does not exist (e.g., for $\rho_v = 0.12$ %), intersections of the curves with a straight line passing through the value of V at $w = 1$ mm for medium friction and parallel to the initial slope of the closest set of curves with a definable initial slope (here $\rho_v = 0.28$ %) are used.

Results are shown in Table 3.

Shear Friction of RC Beams

Fig. 9c shows the RC beam used in this study. The RC beam has the same external dimensions as the PC beam, but the longitudinal reinforcement now consists of 8 #7 bars ($\phi = 22$ mm) top and bottom

and 2 #3 bars ($\phi = 9.5$ mm) at middepth for crack control. The concrete cylinder strength is 43 MPa, and the shear reinforcement, similar to that of the PC beam, also satisfies the ACI requirements ($.094 \% \leq \rho_v \leq 1.2 \%$). Stirrup spacing does not exceed $d/2 = 280$ mm. Stirrups consist of #4 bars ($\phi = 13$ mm), #3 bars ($\phi = 9.5$ mm) or #2 smooth bars ($\phi = 6$ mm) at 152 mm. An additional configuration is #2 bars at 280 mm. These correspond to shear reinforcement ratio of $\rho_v = 1.11 \%$, 0.61% , 0.28% and 0.15% respectively (Table 4). Behavior is similar to that of the PC beam previously described. All beams failed by concrete crushing, the longitudinal reinforcement did not yield. Quantitative comparison is easier here than for the PC beam, because in all cases an initial straight line can be defined and the 1 mm offset method is straightforward. See Table 5 and Fig. 11.

Table 4 Stirrup and Crack Spacing for RC Beam

Stirrup bar #	s mm	ρ_v %	s_{max} mm	s_{mv} mm
2 (smooth)	280	0.15	340	1008
2 (smooth)	152	0.28	340	602
3	152	0.61	336	302
4	152	1.11	333	251

Table 5 Variation of Shear Force V of a RC Beam for Various Values of Shear Friction F and Stirrup Ratio ρ_v .

F	0.27			0.18			0.063			Method
	ρ_v %	θ°	V (kN)	%	θ°	V (kN)	%	θ°	V (kN)	
1.11	31.4	600.4	104	31.3	579.7	100	31.0	546.0	94	1 mm offset
0.61	28.1	412.3	106	28.0	387.2	100	27.7	352.2	91	1 mm offset
0.28	26.3	245.8	111	24.7	221.8	100	26.3	184.3	83	1 mm offset
0.15	24.7	174.6	114	24.9	153.8	100	25.4	118.2	77	1 mm offset
0.28	29.6	260.8	111	20.1	235.3	100	35.0	172.4	73	peak or linear limit
0.15	29.7	206.9	112	31.2	184.0	100	44.0	135.9	74	peak or linear limit

For both the PC and RC beams, the following is observed:

- As the shear reinforcement ratio decreases, the effect of shear friction increases. This is to be expected since, as shear reinforcement decreases, the proportion of shear load carried by shear friction increases. For a shear friction parameter of 35 % of the base case, as in HSC compared

to NSC, the shear force V at or near its peak is 15 % to 25 % lower than for the base case, depending on the method of estimation.

- Two cases were run for the PC beam (for $f'_c = 38.6$ MPa, $\rho_v = 1.11$ % , $F = 0.18$ or 0.063) using the 1986 version of the MCFT, which has a more elaborate shear friction law, Eq. 2, compared with the 1991 version, Eq. 3. The results of the two versions are indistinguishable from one another, i.e., the normal compressive stress σ across shear cracks is negligible.
- Failure by concrete crushing is predicted to occur at high w (very wide cracks), much higher than the range of Walraven's experimental data ($v \leq 2$ mm, $w \leq 1.5$ mm).

Biaxial Softening

Computer program SHEAR was modified by replacing Eqs. 4 and 6 with various biaxial softening models. For the PC beam (Fig. 12), in the cases where SHEAR did not predict concrete crushing, the program was stopped after large crack widths were attained (about 20 mm). The curve shear force versus crack width ceases to be linear shortly after stirrups yield and cracks slip. Peaks (local peaks in some cases) occur near that point and are compared in Table 6. Two types of behavior are observed for the various softening models (Fig. 12 and Table 6):

- Significant post-linear strength gain is predicted by the models of Kollegger, Okamura, Miyahara and Shirai, which predict no concrete crushing (failure is by excessive deformation); and the models of Ueda and Noguchi, which predict fairly similar behavior, concrete crushing after considerable post-linear strength and wide cracks.
- No post-linear strength gain is predicted by the models of Collins, Vecchio-B, and Hsu.

For the RC beam, the various models start deviating from linearity (of the $V-w$ curve) and from each other when stirrups yield, followed shortly afterwards by crack slipping. Two types of behavior are predicted:

- shear compression failure (concrete crushing) is predicted by the models of Collins, Hsu and Vecchio-B.
- shear tension failure (yielding of the longitudinal reinforcement) is predicted by the models of Ueda, Noguchi, Kollegger, Miyahara, Okamura and Shirai. Ueda's model comes close to predicting a balanced failure by both compression and tension.

Results are shown in Table 7.

Table 6 PC Beam: Shear Force for Various Biaxial Softening Laws
 ($\rho_v = 0.61\%$. Subscript L for end of linear range.)

Model	V_L (kN)	w_L (mm)
Kollegger	476	0.8
Shirai	455	0.6
Okamura	465	0.6
Miyahara	438	0.6
Noguchi	460	0.6
Ueda	477	0.8
Hsu	471	0.6
Vecchio-B	459	0.6
Collins	468	0.7

Table 7 RC Beam: Shear Force for Various Biaxial Softening Laws ($\rho_v = 1.11\%$)

Model	V_{max} kN	V_{max} % of smallest	w_{max} mm	At last iteration ($1000 \epsilon_y = 1.83$)			Mode of failure
				f_c MPa	f_{2max} MPa	$1000 \epsilon_x$	
Ueda	454	111	6.3	17.4	19.8	1.81	Tension
Noguchi	454	111	5.2	17.2	25.3	1.78	T
Kollegger	454	111	4.1	17.1	43.0	1.77	T
Miyahara	437	107	3.7	17.3	25.8	1.80	T
Okamura	454	111	5.2	17.3	25.8	1.80	T
Shirai	454	111	5.0	17.4	29.3	1.80	T
Collins	409	100	4.6	13.7	14.1	1.35	Compression
Hsu	429	105	3.1	14.8	15.3	1.47	C
Vecchio-B	426	104	4.14	14.8	17.2	1.48	C

Table 6 PC Beam: Shear Force for Various Biaxial Softening Laws
($\rho_v = 0.61\%$. Subscript L for end of linear range.)

Model	V_L (kN)	V_L/V_x (%)	w_L (mm)
Kollegger	476	111	0.8
Shirai	455	106	0.6
Okamura	465	108	0.6
Miyahara	438	102	0.6
Noguchi	460	107	0.6
Ueda	477	111	0.8
Hsu	471	110	0.6
Vecchio-B	459	107	0.6
Collins	473	110	0.7

Table 7 RC Beam: Shear Force for Various Biaxial Softening Laws ($\rho_v = 1.11\%$)

Model	V_{max} kN	V_{max} % of smallest	w_{max} mm	At last iteration ($1000 \epsilon_y = 1.83$)			Mode of failure
				f_2 MPa	f_{2max} MPa	$1000 \epsilon_x$	
Ueda	454	111	6.3	17.4	19.8	1.81	Tension
Noguchi	454	111	5.2	17.2	25.3	1.78	T
Kollegger	454	111	4.1	17.1	43.0	1.77	T
Miyahara	437	107	3.7	17.3	25.8	1.80	T
Okamura	454	111	5.2	17.3	25.8	1.80	T
Shirai	454	111	5.0	17.4	29.3	1.80	T
Collins	409	100	4.6	13.7	14.1	1.35	Compression
Hsu	429	105	3.1	14.8	15.3	1.47	C
Vecchio-B	426	104	4.14	14.8	17.2	1.48	C

Conclusion

Laws for shear friction and biaxial softening of concrete used in various beam shear theories vary widely. The modified compression field theory (MCFT) was used to study the effects of various shear friction and concrete softening formulations on the calculated shear strength of PC and RC beams. According to the MCFT, a decrease in shear friction within the range of experimental data, as found for example in high strength concrete, lowers the shear strength of beams with low shear reinforcement by 15 % to 25 %, depending on the method of estimation.

In addition, a comparison is presented of different relationships used to represent the biaxial compression-tension strength of reinforced concrete. For PC beams where the prestressing cables do not fail, some theories of biaxial softening of concrete do not predict concrete crushing even for very high deformations. For RC beams, some models predict shear tension failure while others predict shear compression failure. However, the peak shear forces which occur close to stirrup yielding and crack slipping are within 10 % of each other for the various theories and of the test value for the PC beam.

Acknowledgment

Mike P. Collins, Julio A. Ramirez and Nick J. Carino reviewed earlier drafts of this paper and offered valuable suggestions; Wilasa Vichit-Vadakan helped with some of the computer runs and graphics; and Long T. Phan served as Division reviewer. To all, the author extends his thanks.

Notation

A_v	= area of shear reinforcement
a_x, a_y	= projection parallel, perpendicular to crack of contact area between aggregate and mortar
b_w	= beam width
c	= maximum size of aggregate
d	= beam depth, from extreme compression fiber to centroid of tension reinforcement
F	= friction parameter
f_c'	= concrete cylinder strength or uniaxial compressive strength
f_{cc}	= concrete cube strength or uniaxial compressive strength
f_{c1}	= principal tensile stress in concrete web
f_{c2}	= principal compressive stress in concrete web
f_{c2max}	= compressive strength of concrete panel in biaxial tension-compression
f_{c2base}	= uniaxial compressive stress for Thorenfeldt curve
f_{cw}	= compressive strength of concrete web
f_p	= maximum compressive stress for softened concrete
f_t	= concrete tensile strength
f_v	= stress in shear reinforcement
f_{vy}, f_y	= yield strength of shear reinforcement
jd	= beam shear depth

h	= overall section depth
s	= stirrup spacing
s_{mv}	= crack control characteristics of transverse reinforcement
s_{mx}	= crack control characteristics of longitudinal reinforcement
V	= shear force, shear strength
V_c	= concrete contribution to shear strength
V_{ci}	= shear force at flexure-shear cracking
V_{cw}	= shear force at web-shear cracking
V_s	= steel contribution to shear strength
v	= crack slip
v_{ci}, τ	= shear stress at crack interface
w	= crack opening
β	= softening parameter
ϵ_0	= strain at maximum compressive stress for uniaxial compression
ϵ_1	= principal tensile strain in concrete
ϵ_2	= principal compressive strain in concrete
ϵ_{1L}	= concrete tensile strain at which reinforcement at crack begins to yield
ϵ_p	= strain corresponding to f_p
ϵ_y	= yield strain of shear reinforcement
θ	= strut angle
μ	= friction coefficient between aggregate and mortar
ρ_v	= shear reinforcement geometrical ratio
σ	= normal stress across a crack
σ_{pm}	= mortar strength
τ_{f0}	= cohesion friction stress (for $\sigma = 0$)
τ_{max}	= maximum shear stress transmitted across a crack
ϕ	= crack angle, bar diameter
ω	= shear reinforcement mechanical ratio

References

- AASHTO (American Association of State Highway and Transportation Officials) (1994): "LRFD Bridge Design Specifications." 1st ed., Washington, D.C., 1091 pp.
- ACI (American Concrete Institute) (1995): "ACI Building Code Requirements for Reinforced Concrete ." ACI 318-95.
- Bazant, Z. and Gambarova, P. (1980): "Rough Cracks in Reinforced Concrete" ASCE ST 4, v. 106, Apr.1980, pp. 819-841.
- Belarbi, A., and Hsu, T.C. (1995): "Softened Concrete in Biaxial Tension-Compression." ACI St. J., v. 92, no. 5, Sep.-Oct. 1995, pp. 562-573.

h	= overall section depth
s	= stirrup spacing
s_{mv}	= crack control characteristics of transverse reinforcement
s_{mx}	= crack control characteristics of longitudinal reinforcement
V	= shear force, shear strength
V_c	= concrete contribution to shear strength
V_{ci}	= shear force at flexure-shear cracking
V_{cw}	= shear force at web-shear cracking
V_s	= steel contribution to shear strength
V_x	= experimental shear strength
v	= crack slip
v_{ci}, τ	= shear stress at crack interface
w	= crack opening
β	= softening parameter
ϵ_0	= strain at maximum compressive stress for uniaxial compression
ϵ_1	= principal tensile strain in concrete
ϵ_2	= principal compressive strain in concrete
ϵ_{1L}	= concrete tensile strain at which reinforcement at crack begins to yield
ϵ_p	= strain corresponding to f_p
ϵ_y	= yield strain of shear reinforcement
θ	= strut angle
μ	= friction coefficient between aggregate and mortar
ρ_v	= shear reinforcement geometrical ratio
σ	= normal stress across a crack
σ_{pm}	= mortar strength
τ_{fd}	= cohesion friction stress (for $\sigma = 0$)
τ_{max}	= maximum shear stress transmitted across a crack
ϕ	= crack angle, bar diameter
ω	= shear reinforcement mechanical ratio

References

- AASHTO (American Association of State Highway and Transportation Officials) (1994): "LRFD Bridge Design Specifications." 1st ed., Washington, D.C., 1091 pp.
- ACI (American Concrete Institute) (1995): "ACI Building Code Requirements for Reinforced Concrete ." ACI 318-95.
- Bazant, Z. and Gambarova, P. (1980): "Rough Cracks in Reinforced Concrete" ASCE ST 4, v. 106, Apr.1980, pp. 819-841.
- Belarbi, A., and Hsu, T.C. (1995): "Softened Concrete in Biaxial Tension-Compression." ACI St. J., v. 92, no. 5, Sep.-Oct. 1995, pp. 562-573.

- Belarbi, A., and Hsu, T.C. (1991): "Constitutive Laws of RC in Biaxial Tension-Compression." Research Report UHCEE 91-2, Univ. of Houston, Texas.
- Bhide, S.B. and Collins, M.P. (1989): "Influence of Axial Tension on the Shear Capacity of Reinforced Concrete Members." ACI St. J., Sep.-Oct. 1989, pp. 570-581.
- Collins, M.P. and Mitchell, D. (1991): Prestressed Concrete Structures. Prentice-Hall Inc, Englewood Cliffs, N.J., 1991, 766 pp.
- Collins, M.P. and Peeress, A. (1989): "Shear Design for High Strength Concrete." SEB Bull. d'Information no. 193: *Design Aspects of High Strength Concrete*, pp. 75-83. Presented at the 26th Plenary Session of SEB, Dubrovnik, Sep. 1988.
- CSA (Canadian Standards Association) (1994): "Design of Concrete Structures." CSA A23.3-94, Dec. 1994, 200 pp.
- Fréney, J.W. (1990): "Theory and Experiments on the Behavior of Cracks in Concrete Subjected to Sustained Shear Loading." Delft Univ. of Technology, Heron, v. 35, no. 1, 80 pp.
- Fréney, J.W. (1985): "Shear Transfer Across a Single Crack in Reinforced Concrete under Sustained Loading." Part I, Experiments, Stevin Report, 5-85-5, 114 pp.
- Fréney, J.W., Pruijssers, A.F., Reinhardt, H.W. and Walraven, J.C. (1987): "Shear Transfer in High Strength Concrete." Proc. Symp. on *Utilization of High Strength Concrete*, Stavanger, Norway, June 1987, pp. 225-235.
- Hofbeck, J.A., Ibrahim, I.O. and Mattock, A.H. (1969): "Shear Transfer in Reinforced Concrete." ACIJ, v.66, no. 2, Feb. 1969, pp. 119-128.
- Hognestad, E. (1952): "What do we know about Diagonal Tension and Web Reinforcement in Concrete ?" Univ. of Illinois Engrg. Exp. Station, Circular Series no.64, 47 pp.
- Hsu, T. (1993): Unified Theory of Reinforced Concrete. CRC Press, 1993, 313 pp.
- Joint ASCE-ACI Task Com. 426 on Shear and Diagonal Tension (1973,1990): "The Shear Strength of Reinforced Concrete Members." J. Struct. Div., ASCE ST6, June 1973, reapproved 1990.
- Kollegger, J. and Mehlhorn, G. (1990): "Material Model for the Analysis of RC Surface Structures." Computational Mechanics, no. 6, pp. 341-357, Springer Verlag.
- Kollegger, J. and Mehlhorn, G. (1987): "Material Model for Cracked RC." IABSE Colloq. on *Computational Mechanics of Concrete Structures: Advances and Applications*, Delft, Report no. 54, pp. 63-74.

Kupfer, H. and Bulicek, H. (1992): "A Consistent Model for the Design of Shear Reinforcement in Slender Beams with I- or Box-Shaped Cross-Section." Proc. Symp. on *Concrete Shear in Earthquake*, Houston, pp. 256-265.

Kupfer, H., Mang, R. and Karavesyoglou, M. (1983): "Ultimate Limit State of the Shear Zone of Reinforced and Prestressed Concrete Girders - An Analysis taking Aggregate Interlock into Account." *Bauingenieur* 58, pp. 143-149, (In German).

MacGregor, J.G. (1992): Reinforced Concrete: Mechanics and Design. 2nd ed., Prentice Hall, Englewood Cliff, N.J., 1992, 848 pp.

Mau, S.T. and Hsu, T.T. (1988): Discussion of paper by Walraven, J.C., Fréney, J. and Pruijssers, A. (1987): "Influence of Concrete Strength and Load History on the Shear Friction Capacity of Concrete Members." *PCIJ*, v. 22, no. 1, Jan.-Feb. 1988, pp. 166-170.

Mikame, A., Uchida, K. and Noguchi, H. (1991): "A Study of Compressive Deterioration of Cracked Concrete." Proc. Int. Workshop on *FEA of RC*, Columbia Univ., New York, N.Y.

Miyahara, T., Kawakami, T. and Maekawa, K. (1988): "Non Linear Behavior of Cracked RC Plate Element under Uniaxial Compression." Proc. Japan Society of Civil Engineers, v. 11, pp. 306-319. Also in *Concrete Library Int.*, JSCE, no. 11, June 1988, pp. 131-144.

Norwegian Council for Building Standardization (1992): Norwegian Standard NS 3473 E, 4th ed., Nov. 1992.

Paulay, T., Loeber, P.J. (1974): "Shear Transfer by Aggregate Interlock." ACI SP 42.1: *Shear in Reinforced Concrete*, pp. 1-15.

Poli, S.D., Prisco, M.D. and Gambarova, P.G. (1990): "Stress Fields In Web of Reinforced Concrete Thin-Webbed Beams Failing in Shear." *J. Struct. Engrg.*, v. 116, no. 9, Sept. 1990, pp. 2496-2515.

Prisco, M.D. and Gambarova, P.G. (1995): "Comprehensive Model for Study of Shear in Thin-Webbed RC and PC Beams ." *J. Struct. Engrg.*, v. 121, no. 12, Dec. 1995, pp. 1822-1831.

Prujssers, A.F., and Liqui Lung, G. (1985): "Shear Transfer Across a Crack in Concrete Subjected to Repeated Loading - Experimental Results." Part I, Stevin Report 5-85-12, 178 pp.

Reineck, K.H. (1991): "Modeling of Members with Transverse Reinforcement." IABSE Colloq. on *Structural Concrete*, Stuttgart, IABSE Rep., v. 62, pp. 481-488.

Reineck, K.H. (1982): "Models for the Design of Reinforced and Prestressed Concrete Members." Part 2 of Progress Report of Task Group IV/1 *Shear in Prestressed Concrete* SEB Bull. d'Information no. 146, Jan. 1982.

- Shirai, S. and Noguchi, H. (1989): "Compressive Deterioration of Cracked Concrete." *Structures Congress: Design, Analysis and Testing*, Proc. ASCE, New York, N.Y., pp. 1-10.
- Tanabe, T., and Wu, Z. (1991): "Strain Softening under Biaxial Tension and Compression." IABSE Colloq. on *Structural Concrete*, Stuttgart, IABSE Reports, v. 62, pp. 623-636.
- Thorenfeldt, E., Tomaszewicz, A. and Jensen, J.J. (1987): "Mechanical Properties of HSC and Application in Design." Proc. Symp. on *Utilization of HSC*, Stavanger, Norway, June 1987, pp. 149-159.
- Ueda, M., Noguchi, H., Shirai, N. and Morita, S. (1991): "Introduction to Activity of new RC." Proc. Int. Workshop on *FEA of RC*, Columbia Univ., New York, N.Y.
- Vecchio, F.J. and Collins, M.P. (1993): "Compression Response of Cracked Reinforced Concrete." ASCE J. St. Engrg., v. 119, no. 12, Dec. 1993, pp. 3590-3610.
- Vecchio, F.J. and Collins, M.P. (1986): "The Modified Compression Field Theory for Reinforced Concrete Elements Subjected to Shear." ACIJ. v. 83, no. 2, March-April 1986, pp. 219-231.
- Vecchio, F.J. and Collins, M.P. (1982): "The Response of Reinforced Concrete to In-Place Shear and Normal Stresses." Pub 82.03, Dept. of Civil Engineering, Univ. of Toronto, March 1982, 332 pp.
- Vecchio, F.J., Collins, M.P. and Aspiotis, J. (1994): "High Strength Concrete Elements Subjected to Shear." ACI St. J., Jul.-Aug. 1994, pp. 423-433.
- Walraven, J.C. (1995): "Shear Friction in High Strength Concrete." *Progress in Concrete Research*, Delft University of Technology, v. 4, pp. 57-65.
- Walraven, J.C. (1981): "Fundamental Analysis of Aggregate Interlock." J. Struct. Div., ASCE, v. 107, ST11, November 1981, pp. 2245-2270.
- Walraven, J.C., Fréney, J. and Pruijssers, A. (1987): "Influence of Concrete Strength and Load History on the Shear Friction Capacity of Concrete Members." PCIJ. v. 32, no. 1, Jan.-Feb. 1987, pp. 66-85.
- Walraven, J.C. and Reinhardt, H.W. (1981): "Theory and Experiments on the Mechanical Behavior of Cracks in Plain and Reinforced Concrete Subjected to Shear Loading." *Heron* v. 26, no. 1A, 68 pp.
- Walraven, J. and Stroband, J. (1994): "Shear Friction in High-Strength Concrete." Proc. ACI Int. Conf. on *High Performance Concrete*, Singapore, ACI SP 149-17, pp. 311-330.

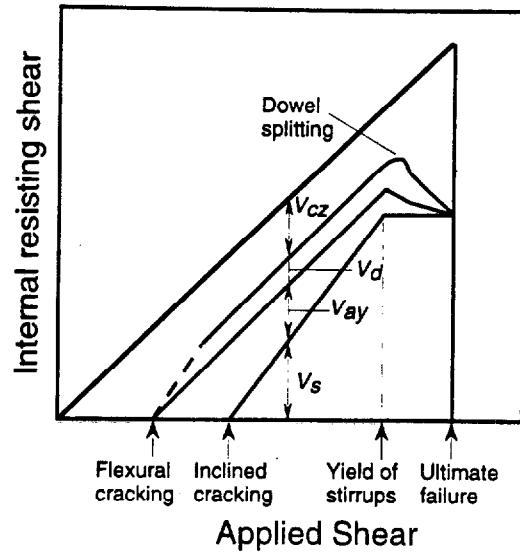
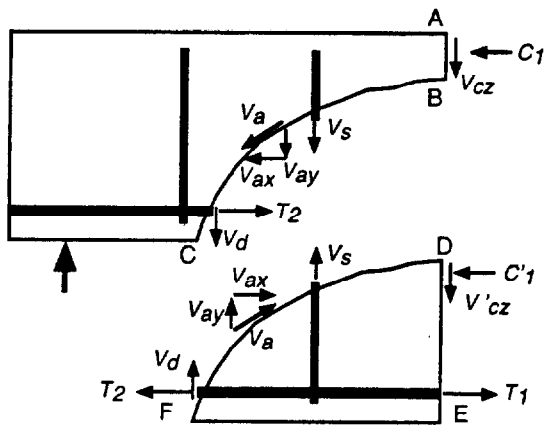


Fig. 1 - (a) Internal forces in cracked beam with stirrups; (b) relative magnitude of shear carrying mechanisms: V_s due to stirrups; V_{ay} due to aggregate interlock; V_d due to dowel action; and V_{cz} due to compression zone of beam (adapted from MacGregor 1992).

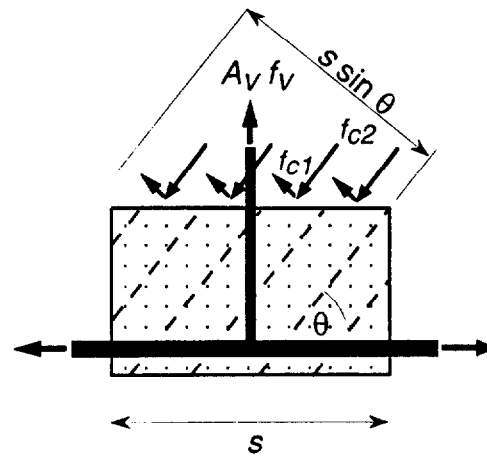
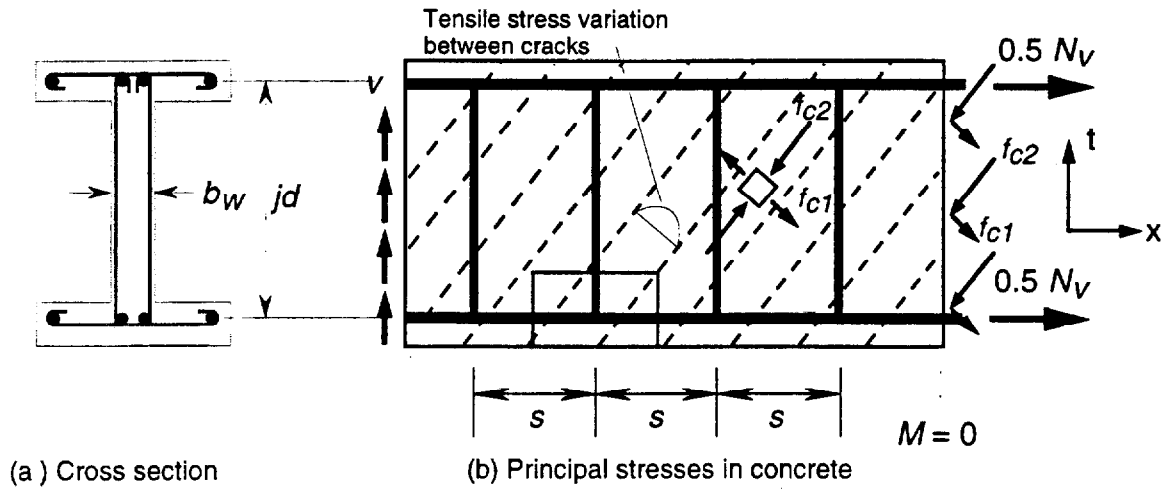


Fig. 2 - Equilibrium conditions for modified compression field theory (Collins and Mitchell 1991).

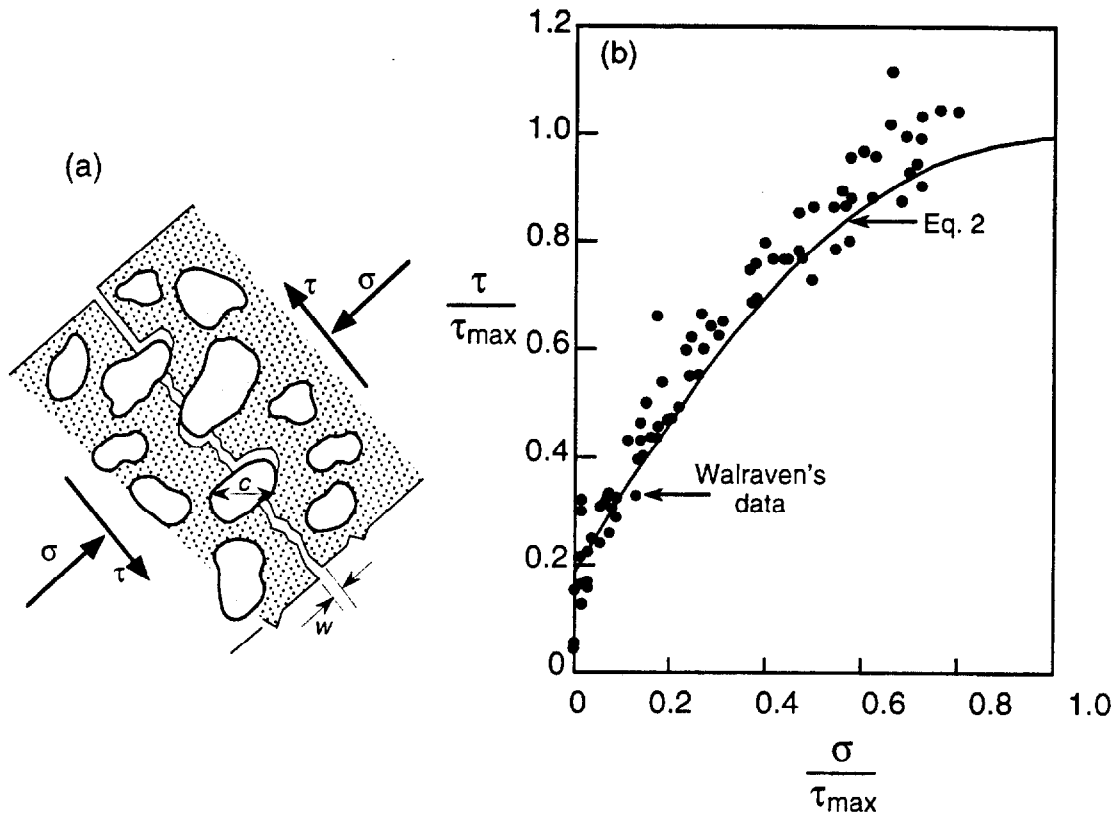


Fig. 3 - (a) Transmission of shear stress across crack by aggregate interlock;
 (b) relationship between shear stress transmitted across crack and
 compressive stress on crack (adapted from Vecchio and Collins 1986)

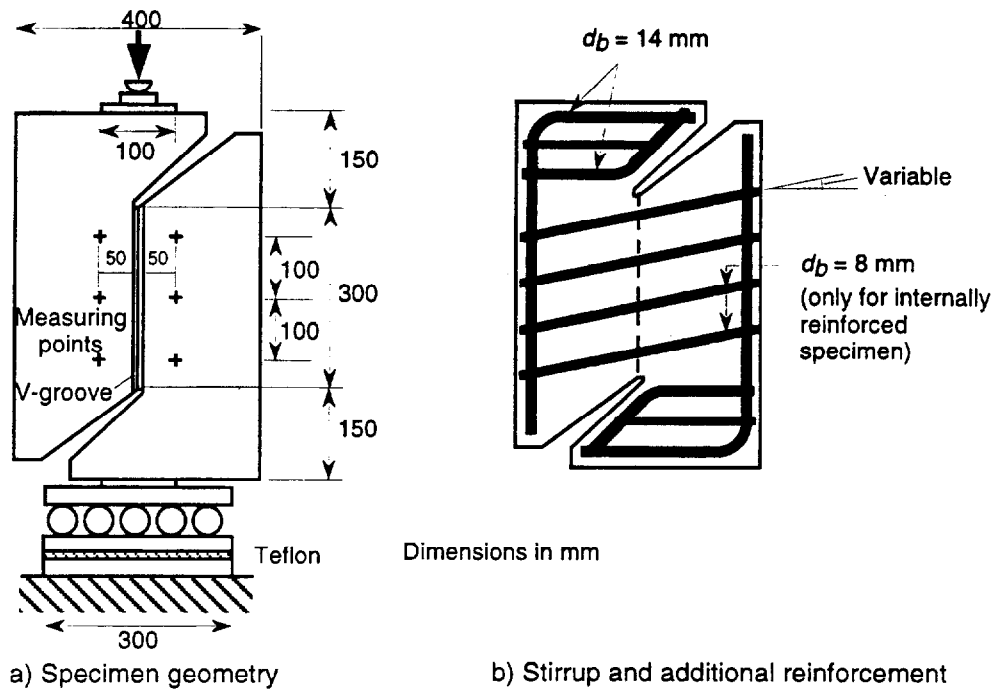


Fig. 4 - Push-off test specimens to study aggregate interlock in cracked reinforced concrete: (a) geometry ; (b) reinforcement (Walraven and Reinhardt 1981)

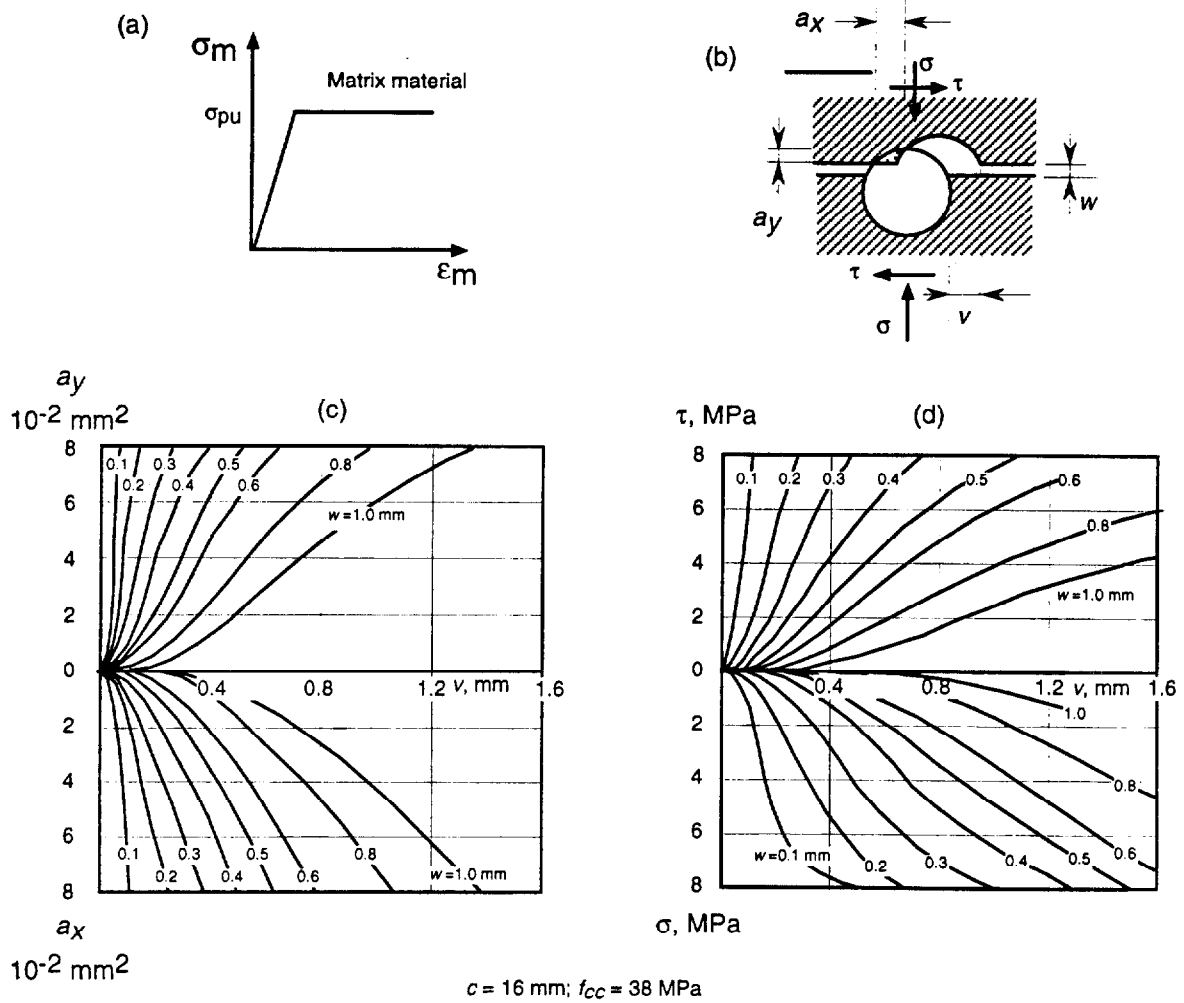


Fig. 5 - Walraven's model for shear transfer across crack: (a) stress-strain curve of matrix material; (b) deformation at crack; (c) contact areas as functions of crack width and slip; and (d) normal and shearing stresses as functions of crack width and slip (adapted from Fréney 1990)

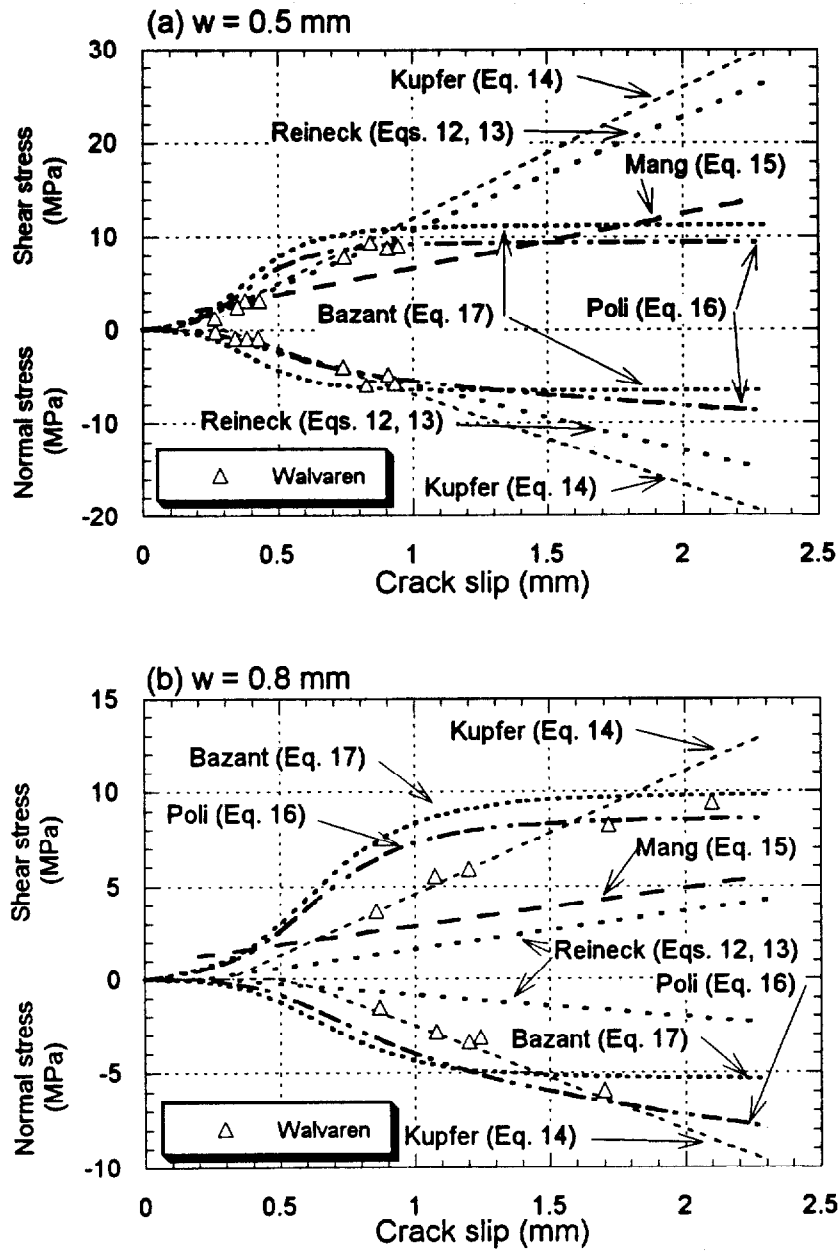


Fig. 6 - Crack behavior according to various researchers

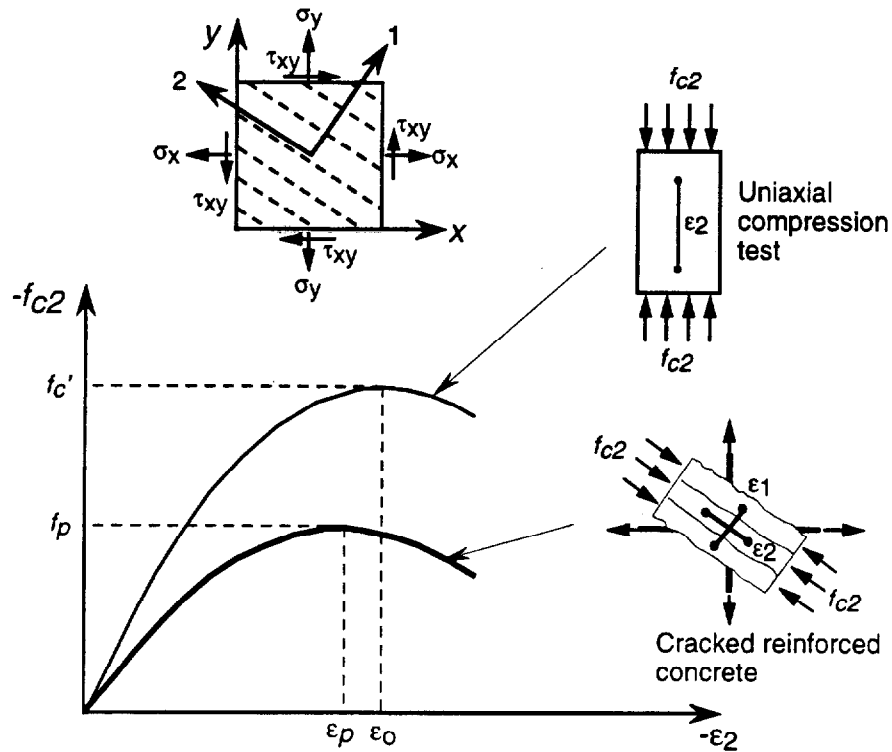


Fig. 7 - Deteriorated compression response in cracked reinforced concrete elements (Vecchio and Collins 1993).

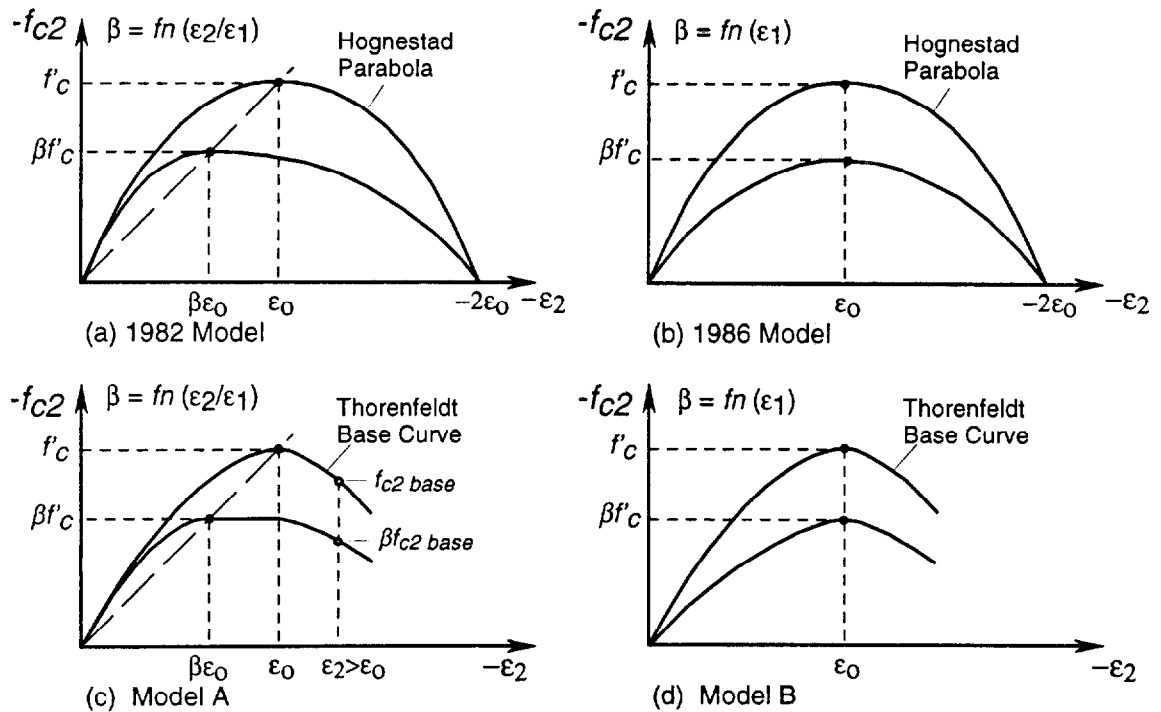
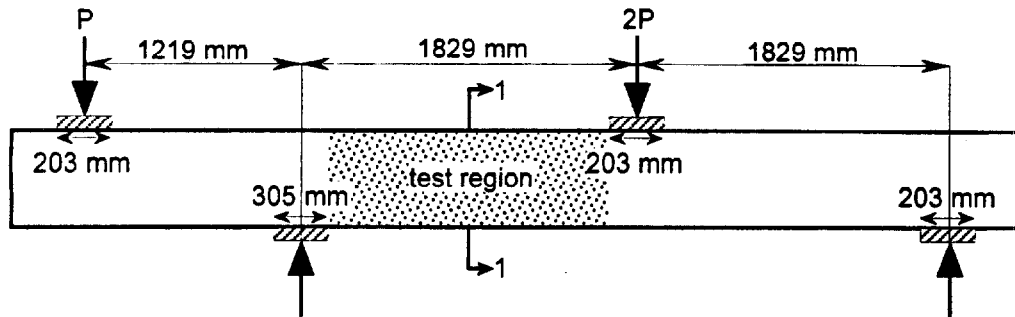
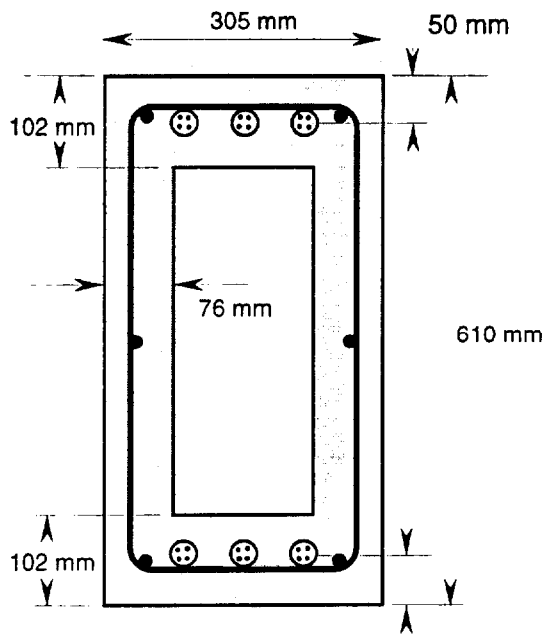


Fig. 8 - Compression softening models: (a) 1982 model; (b) 1986 model; (c) proposed model A; and (d) proposed model B (Vecchio and Collins 1993).

(a) Test beam



(b) Section 1-1 of PC beam



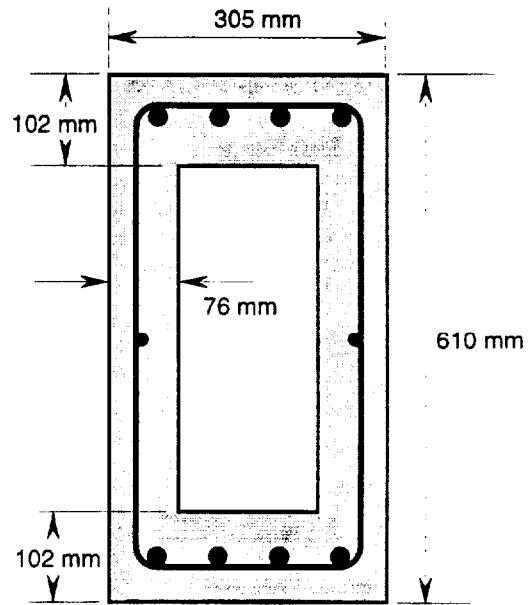
Cover:
side = 13 mm
top & bottom = 25 mm

$f'_c = 38.6$ MPa

Mild steel reinforcement:
stirrups = 9.5 mm dia. @ 152 mm
longitudinal = 6 x 9.5 -mm dia.
 $f_y = 367$ MPa

Prestressing steel:
6 x 4, 7-mm wire
 $f_{py} = 1450$ MPa
 $f_{pu} = 1680$ MPa
 $\Delta\epsilon_p = 0.0054$

(c) Section 1-1 of RC beam



Cover:
side = 13 mm
top & bottom = 25 mm

$f'_c = 43$ MPa

Reinforcement:
stirrups = 9.5 mm dia. @ 152 mm
longitudinal = 8 x 22 mm dia. (top & bottom)
plus 2 x 9.5 mm dia. (side)
 $f_y = 367$ MPa

Fig. 9 – Configuration of beams used in the parametric study: (a) load configuration, (b) PC beam CF1, and (c) RC beam (adapted from Collins and Mitchell 1991)

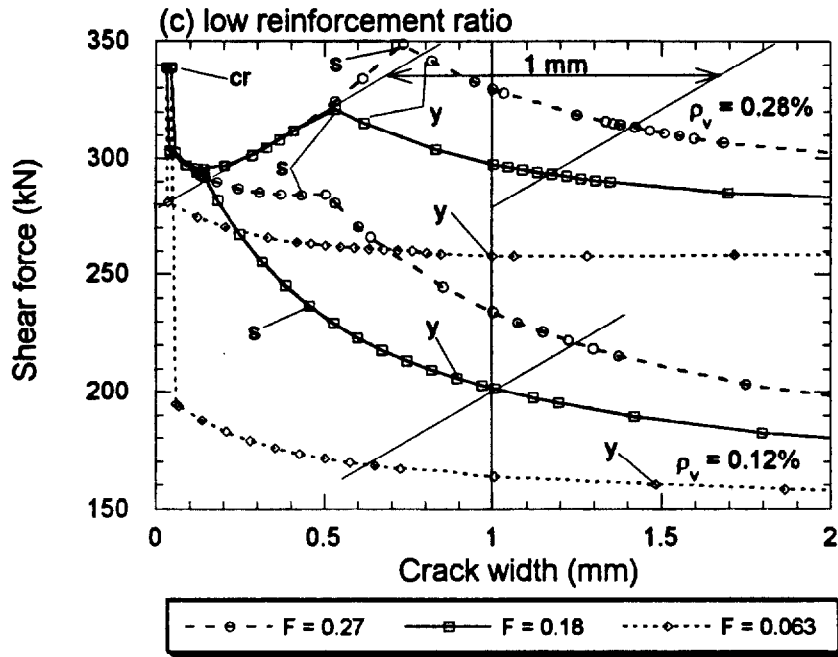


Fig. 10 - Effect of shear friction and shear reinforcement on prestressed concrete beam behavior (cr = initial cracking; y = stirrups yield; s = cracks slip; c = concrete crushes) ($f'_c = 38.6$ MPa)

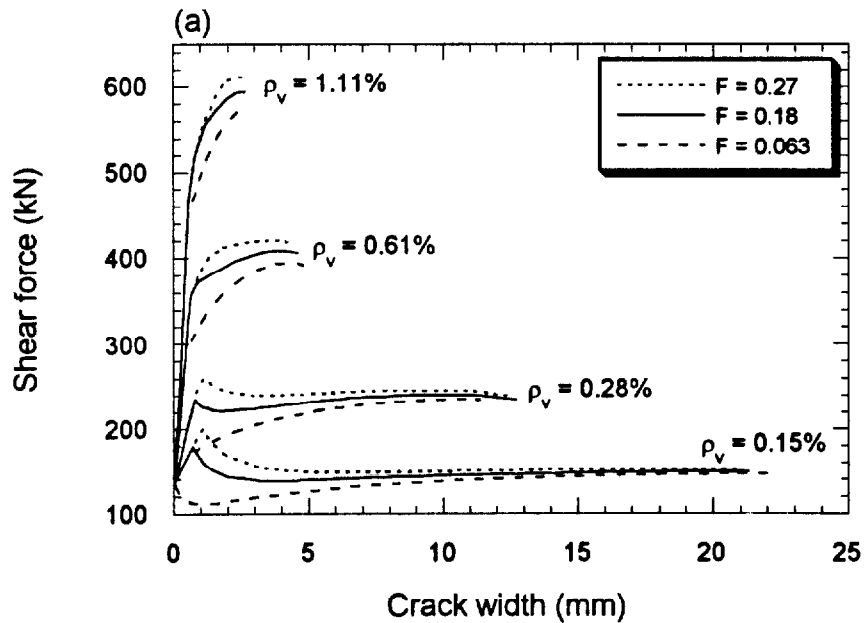


Fig. 11 - Effect of shear friction and shear reinforcement on reinforced concrete beam behavior ($f'_c = 43$ MPa)

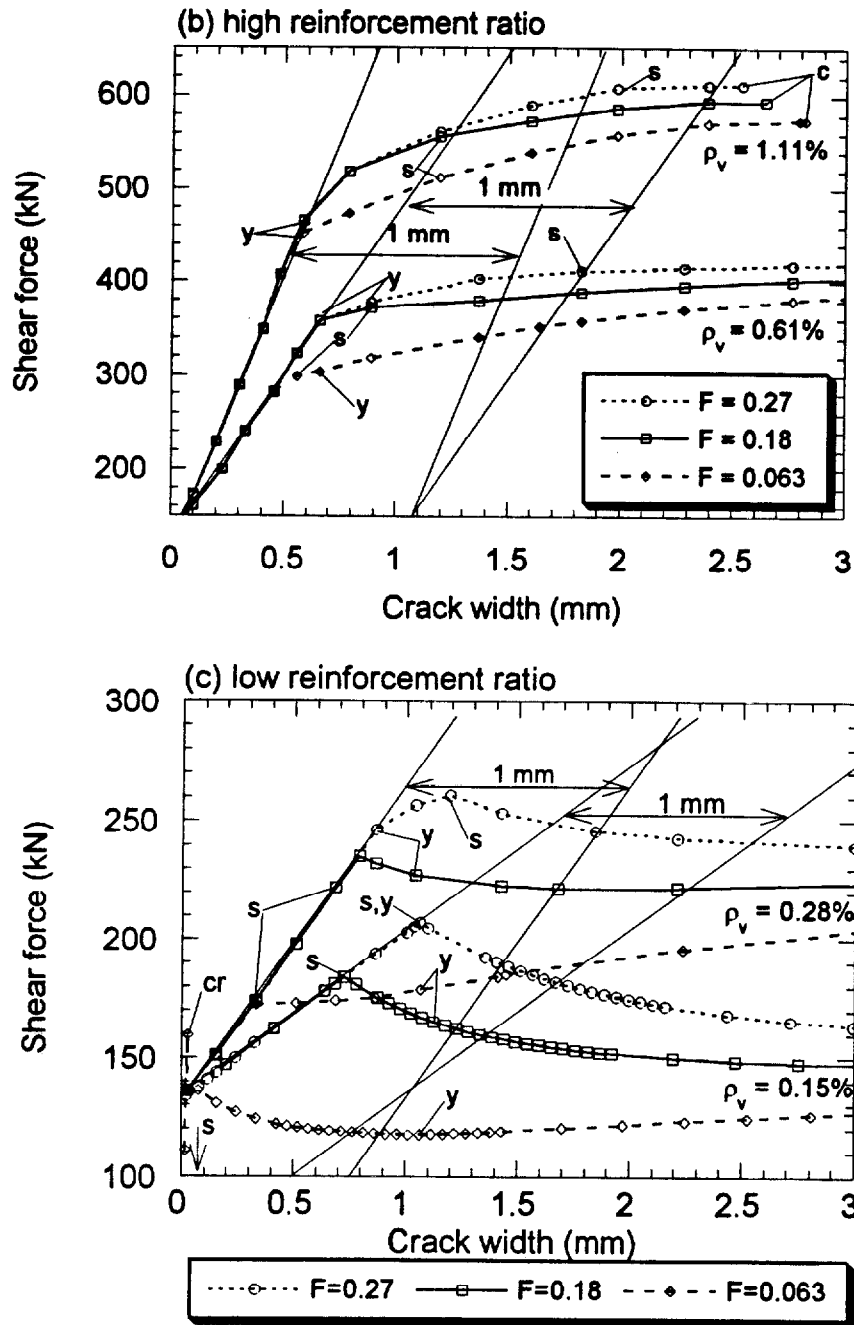


Fig. 11 - Effect of shear friction and shear reinforcement on reinforced concrete beam behavior
 (cr = initial cracking; y = stirrups yield; s = cracks slip; c = concrete crushes)
 ($f'_c = 43$ MPa)

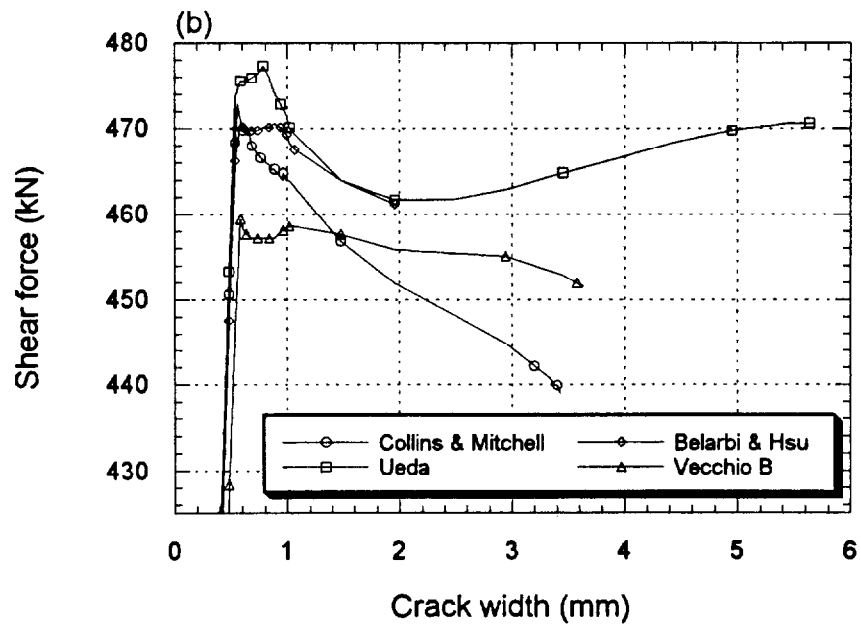
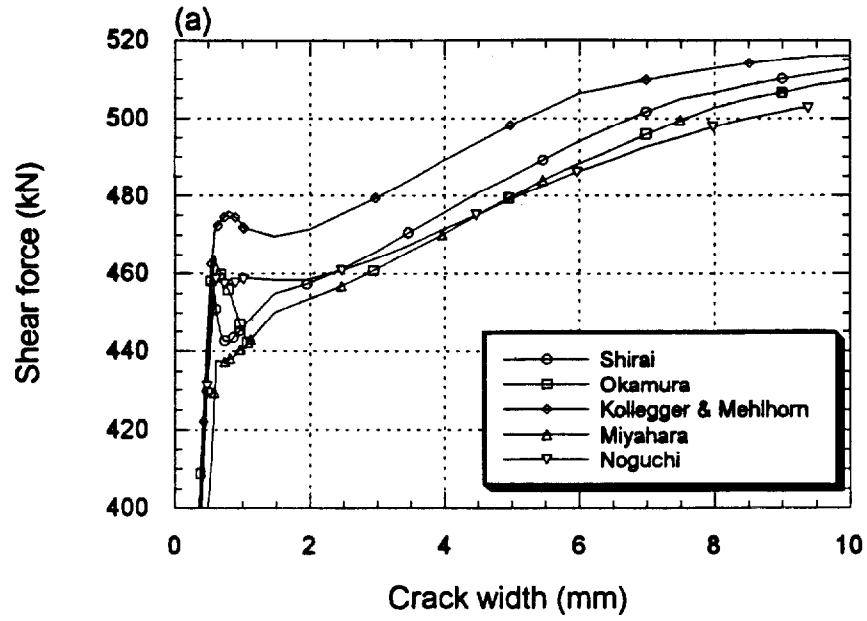


Fig. 12 - Effect of concrete biaxial softening on shear behavior of prestressed concrete beam

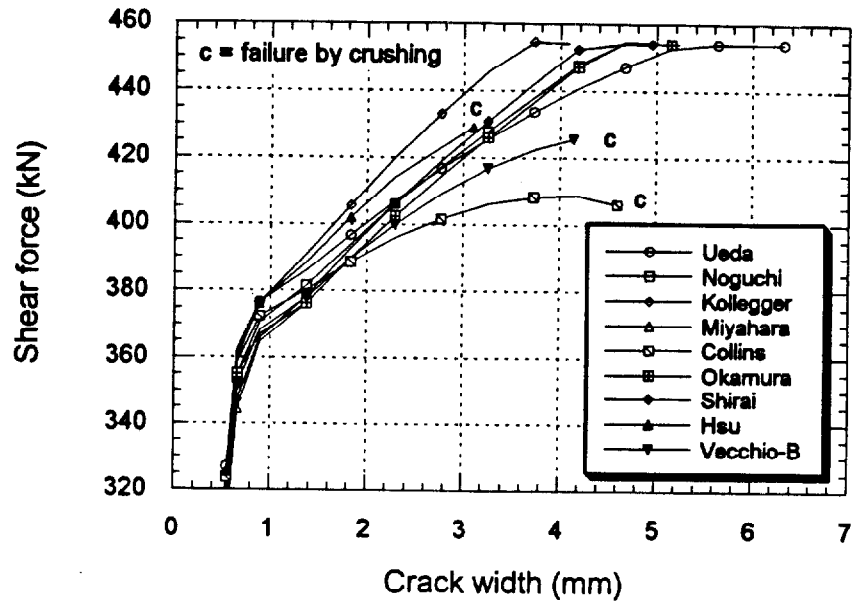


Fig. 13 - Effect of concrete biaxial softening on shear behavior of reinforced concrete beam